Carbohydrate Research 344 (2009) 1745–1752

Contents lists available at ScienceDirect

Carbohydrate Research

journal homepage: www.elsevier.com/locate/carres

Conformational properties of the disaccharide building units of hyaluronan

Peter Pogány [a], Attila Kovács [b,*]

[a] Faculty of Chemical Technology and Biotechnology, Budapest University of Technology and Economics, H-1111 Budapest, Műegyetem rkp. 3, Hungary
[b] Research Group for Materials Structure and Modeling of the Hungarian Academy of Sciences, Department of Inorganic and Analytical Chemistry, Budapest University of Technology and Economics, H-1111 Budapest, Szt. Gellért tér 4, Hungary

ARTICLE INFO

Article history:
Received 17 March 2009
Received in revised form 22 May 2009
Accepted 31 May 2009
Available online 6 June 2009

Keywords:
Hyaluronan
DFT computations
Conformation
Hydrogen bonding
NBO analysis

ABSTRACT

The conformational space of the disaccharide building units of hyaluronan, β-(1→4) and β-(1→3)-linked *N*-acetyl-β-D-glucosamine (**GN**) and β-D-glucuronic acid (**GA**), has been investigated by density functional theory calculations at the B3LYP/6-31G** level. The study covered the anionic disaccharides, the neutral acids as well as the sodium salts in the isolated state and in aqueous solution using the PCM model approach. We elucidated the intramolecular hydrogen bonding interactions characterizing the most favoured conformers. The protonation and salt formation change these secondary interactions in the vicinity of the carboxyl group, resulting often in a considerable alteration of the conformational preferences. The Na^+ ion in the salt is involved in multiple bonding in the most stable structures: beyond the primary ionic bond with the carboxylate group it forms slightly weaker interactions with neighbouring oxygens. The main effect of protonation and salt formation on the electron density distribution is restricted to the surroundings of the broken/formed interactions near the carboxylate group.

1. Introduction

Hyaluronan is a linear glycosaminoglycan polymer of the extracellular matrix consisting of repeating units of the disaccharide [-β-D-glucuronic acid-β-(1→3)-*N*-acetyl-β-D-glucosamine-β-(1→4)-]$_n$. The compound is synthesized in mammals and is formed in varying chain lengths. The chains can decompose by enzymatic reactions resulting in polymers of smaller sizes. Hyaluronan fragments have numerous and often opposing biological functions. For example, large hyaluronan polymers have space-filling, anti-angiogenic, immunosuppressive roles in mammalian bodies and are involved in ovulation, embryogenesis, epithelial layer protection, wound repair and regeneration. The smaller fragments have inflammatory, immuno-stimulatory and angiogenic properties. The tetrasaccharides are known to be anti-apoptotic and inducers of heat shock proteins. Some fragments can trigger signal transduction pathways.[1–4]

The primary structure of hyaluronan is very simple, thus its wide-ranging biological functions are strongly determined by the tertiary structure in the respective matrix, the degree of polymerization, the salt/acidic character and in the case of salts, by the cation. The importance of the structure initiated numerous structural investigations of the polymer[5–9] including crystal structure[10–22], solution NMR[23–29] and molecular modelling studies.[25,30–38]

In spite of the extensive research on this topic, our understanding of the rules governing the structural relations of this saccharide is limited.[5] Even the structural properties of the small oligomers are poorly understood. From the two monosaccharides *N*-acetyl-β-D-glucosamine (**GN**) and β-D-glucuronic acid (**GAH**, Fig. 1) only the structure of the α anomer of **GN** has been reported from X-ray diffraction investigations.[39] In addition, limited computational studies have been performed on selected structures of the mono-, di- and trisaccharide blocks of hyaluronan at low (AM1, HF/3-21G) levels of theory.[40] Conformational properties restricted to the variation of the glycosidic torsional angles Φ and Ψ were also studied for the anionic, neutral and sodium salt of the β-(1→3)-linked disaccharide using molecular mechanics force fields.[41] These latter computed results were in good agreement with average interatomic distances determined by previous NMR measurements in the aqueous solution of the salt. Using a fixed hydrogen bonding pattern, protonation and salt formation were found to have negligible effects on the glycosidic torsional angles and only a minor influence on the relative energies of the conformers.[41] Recently, a detailed conformational analysis of neutral **GAH** was performed by us using the B3LYP/6-311++G** level, where we elucidated the intramolecular interactions determining the conformational preferences of the **GAH** molecule.[42]

The aim of our present study is to extend our knowledge on the structural chemistry of hyaluronan by elucidating structural characteristics of the disaccharide building blocks. Note that our study does not cover the complete conformational space of the disaccharides as we did not perform a full conformational search. We

* Corresponding author. Tel.: +36 1 463 2278; fax: +36 1 463 3408.
E-mail address: akovacs@mail.bme.hu (A. Kovács).

0008-6215/$ - see front matter © 2009 Elsevier Ltd. All rights reserved.
doi:10.1016/j.carres.2009.05.030

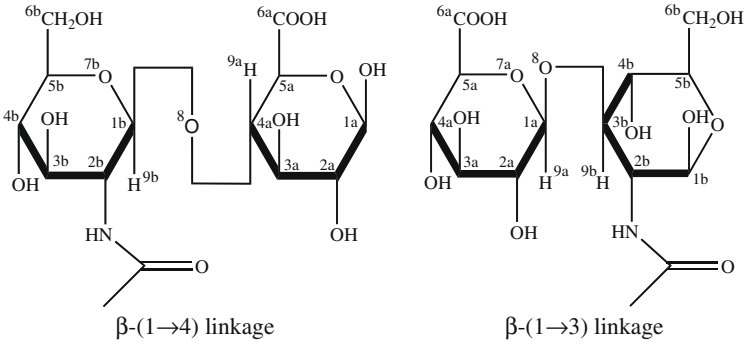

Figure 1. The disaccharide unit of hyaluronan consisting of *N*-acetyl-β-D-glucosamine and β-D-glucuronic acid; CH hydrogens are not shown.

focussed on potential low-energy conformers taking into account among other structural information available on the polymer from previous X-ray[17–19] and on the β-(1→3)-linked disaccharide from molecular mechanics[41] studies. These literature results consist mainly of skeleton structural data while lacking accurate information on the orientation of the OH groups and their interactions. We investigated the possible orientations of the substituents on the pyranose rings of the disaccharides with particular interest in the governing hydrogen bonding interactions and their change upon protonation and salt formation. Therefore, our study included the anion, the neutral acid (hyaluronic acid) and the sodium salt (appearing most frequently in biological systems). We optimized the geometries of the selected structures using density functional theory (DFT). The effect of solvent on the structural properties was modelled using the polarized continuum PCM model.

The designation of the conformers throughout the paper is the following: **GN** and **GAH** indicate the neutral *N*-acetyl-β-D-glucosamine and β-D-glucuronic acid moieties, respectively. The designation **GA** refers to the deprotonated β-D-glucuronic acid, while **GANa** to its sodium salt. The disaccharides can be formed by β-(1→4) and β-(1→3) attachment of the monosaccharides. The two forms are distinguished here by the sequence of the monosaccharide units in the designations (**GN–GA** and **GA–GN**, respectively). The conformers of a disaccharide are ordered according to their relative stability in terms of Gibbs free energies of the isolated structures, the ordering indicated by Arabic numbers at the end of the designations.

2. Computational details

Our quantum chemical computations were carried out using the GAUSSIAN03 suite of programs[43] at the Becke3–Lee–Yang–Parr (B3LYP) level[44,45] in conjunction with a 6-31G** basis set. The minimum character of the stationary points obtained by full geometry optimizations was confirmed by frequency calculations. Gibbs free energies were computed using the rigid-rotor harmonic approximation implemented in GAUSSIAN03. Solvent effects were considered by the polarizable continuum model PCM.[46–48] Note that the solvation energies could be calculated only on the optimized geometries of the isolated structures, as geometry optimizations with the PCM model failed to converge. For evaluation of the atomic charges the Natural Bond Orbital scheme was applied using the NBO5.0 code.[49]

3. Results and discussion

A crucial point of the present study was the selection of the proper structures. We limited our model structures on the type of pyranose rings ($^4C_1$ chair) and β-anomers present in hyaluronan.[31,34,50] The initial structures for the geometry optimizations were constructed manually. Part of the initial glycosidic torsional angles Φ and Ψ between the **GA** and **GN** moieties of the disaccharides was taken from the conformational search of Miertus et al.[41] However, to elucidate the possible strong inter-monosaccharide hydrogen bonding interactions, we extended the inspected ranges of Φ and Ψ torsionals beyond the values reported by Miertus et al.[41] The determination of the favoured orientations of the OH and acetylamino groups was carried out in the following way: It can be assumed, that in the gaseous phase the conformers possessing the most possible intramolecular hydrogen bonds have the lowest energies. Information on the governing properties of intramolecular hydrogen bonds was available for β-D-glucuronic acid from our recent theoretical study.[42] However, data on the hydrogen bonding in *N*-acetyl-β-D-glucosamine have not been reported hitherto. Therefore, in the first phase of this study we calculated and analyzed several structural possibilities for the disaccharides and used the found favoured orientations of the polar groups (and positions of the sodium ion in the case of salts) to construct the potential lowest-energy conformers. The end effects (effects of neighbouring disaccharides in the hyaluronan polymer) were considered by methyl groups terminating the respective linking oxygen atoms of our model structures.[24,31,51] The Cartesian coordinates of all the computed structures are given as Supplementary data.

3.1. Anions

We start our discussion with the anions, as these structures can serve as parents for investigation of the effects of protonation in the neutral acids as well as that of sodium in the salts. The most stable anion structures including the characteristic hydrogen bonding interactions are presented in Figure 2.

We compared first the two linking types β-(1→4) and β-(1→3) on the basis of the absolute energies of the **GN–GA** and **GA–GN** disaccharides, respectively. This assessment showed that neither β-(1→4) nor β-(1→3) has a general preference for these anionic disaccharides and the relative stability can change upon the influence of thermal contributions and entropy effects (reflected by the Gibbs free energies) as well as upon the solvent. In terms of potential, Gibbs free and solvated Gibbs free energies the most stable structures are **GA–GN1**, **GN–GA1** and **GA–GN5**, respectively.

Analyzing the lowest-energy conformers from the point of view of their relative Gibbs free energies we found that four **GN–GA** and six **GA–GN** conformers fell in the energy window of 20 kJ/mol (cf. Table 1). The depicted most stable **GN–GA** and **GA–GN** conformers differ generally in the interactions (orientations) of the CH_2OH and/or OCH_3 groups. Another significant difference observed in the **GA–GN3**–**GA–GN6** series is the **GN** ring turned over as compared to **GA–GN1** and **GA–GN2**.

The glycosidic linkage of the conformers is characterized by the Φ and Ψ torsionals presented in Figure 1. The torsionals of the

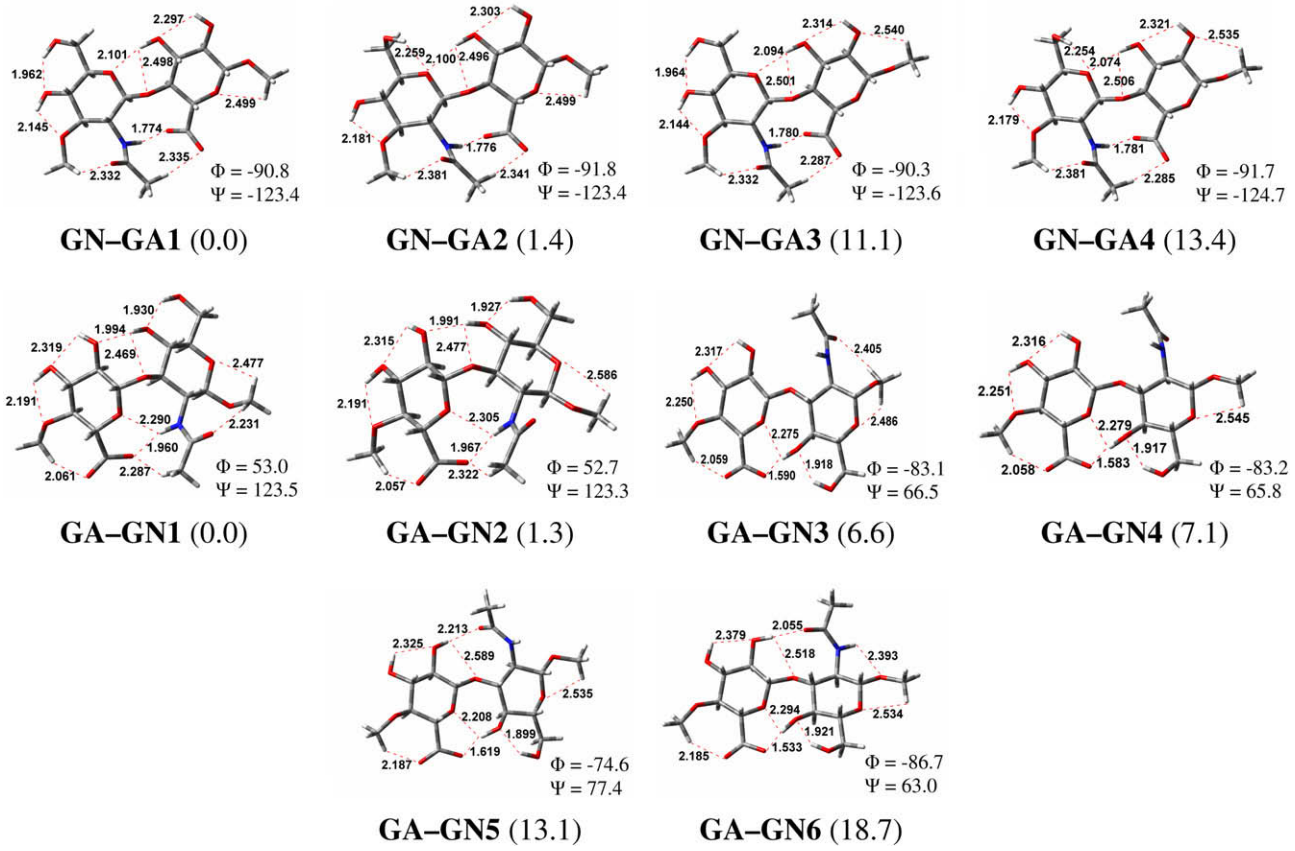

Figure 2. The most stable anionic **GN–GA** and **GA–GN** disaccharides. The computed relative Gibbs free energies in vacuum (kJ/mol) are given in parentheses. The hydrogen bond distances are given in Å. The torsionals are defined as follows: $\Phi = {}^{7a}O{-}{}^{1a}C{-}{}^{8}O{-}{}^{3b}C$ and $\Psi = {}^{1a}C{-}{}^{8}O{-}{}^{3b}C{-}{}^{4b}C$ (for 1→3-linked disaccharides); $\Phi = {}^{7b}O{-}{}^{1b}C{-}{}^{8}O{-}{}^{4a}C$ and $\Psi = {}^{1b}C{-}{}^{8}O{-}{}^{4a}C{-}{}^{5a}C$ (for 1→4-linked disaccharides). For numbering of atoms see Figure 1.

Table 1
Computed relative energies (ΔE), Gibbs free energies in vacuum under standard conditions (ΔG°) as well as in aqueous solution (ΔG°_{aq}) of the most stable anionic **GN–GA** and **GA–GN** disaccharides given in kJ/mol

Name	ΔE	ΔG°	ΔG°_{aq}
GN–GA1	0.0	0.0	6.8
GN–GA2	4.5	1.4	0.0
GN–GA3	14.0	11.1	12.3
GN–GA4	18.2	13.4	6.6
GA–GN1	0.0	0.0	16.7
GA–GN2	5.5	1.3	8.0
GA–GN3	11.6	6.6	12.1
GA–GN4	14.5	7.1	2.7
GA–GN5	22.2	13.1	0.0
GA–GN6	27.1	18.7	13.8

listed **GN–GA** conformers are in good agreement with the respective values of the β-(1→4) linkages measured for crystalline Ca and Na salts of hyaluronan.[17–19] Regarding the **GA–GN1** and **GA–GN2** structures the Ψ torsionals are in good agreement with the crystal structure data of β-(1→3) linkages,[17–19] while the Φ values deviate by ca. 100°. The crystal glycosidic torsionals resemble more the (in the gaseous phase) less stable **GA–GN3** and **GA–GN6** structures, but even here we observed deviations of 30–50° between the computed and X-ray data. Test calculations indicated that the torsionals found in the crystal structure are not favoured for the latter isolated anions, as optimizations starting from the experimental values converged either to one of the listed optimized structures, or to a higher-lying local minimum. A similar situation was observed upon comparison with NMR data:[11] the agreement was good for the β-(1→4) torsionals, while some deviations were found for the β-(1→3) torsionals.

The most characteristic intramolecular interactions in the disaccharides are the hydrogen bonds contributing considerably to the relative stabilities of the conformers. Therefore the most favoured structures possess always a large number of strong hydrogen bonds. One characteristic interaction in the anions is the strong hydrogen bond between the NH hydrogen and one of the carboxylate oxygens (with NH···O distances around 1.77 and 1.96 Å in **GN–GA** and **GA–GN**, respectively). This is the strongest hydrogen bond except for conformers **GA–GN3** to **GA–GN6**, where the strongest interaction appears between the COO and ^{4}OH groups (1.53 and 1.62 Å).

A characteristic difference between the two types of disaccharides is that there are three hydrogen bonds connecting the two monosaccharide moieties in the most preferred **GN–GA** conformers, while the most stable **GA–GN** forms show four such intermoiety hydrogen bonds, where the NH donor is involved in bifurcated interaction. In addition, a very weak (close to the sum of the van der Waals radii) interaction can be observed between the oxygen connecting the two pyranose rings and an OH group having a suitable orientation. We note also the numerous CH···O hydrogen bonds found in all the structures, which are though weak, but they can gain importance (together with other weak interactions) when comparing conformers with close relative energies.

A good example for the effect of the latter weak interactions beyond hydrogen bonding is demonstrated by the conformers **GN–GA1** and **GN–GA3** in Figure 1. **GN–GA3** is less stable by 11.1 kJ/mol than **GN–GA1**, while the only noticeable structural difference is the orientation of the OCH_3 group of the **GA** moiety. The methyl

hydrogens form a similar-strength weak C–H···O interaction in both conformers, hence hydrogen bonding cannot be responsible for the relatively large energy difference. A closer inspection of the three-dimensional structures showed two weak interactions that lead to the preference of **GN–GA1**: one of them is a favourable dipole–dipole interaction between the methyl C–H and ring C–O bonds in **GN–GA1** while the other one is the repulsion of the lone pairs of the methoxy and ring oxygens in **GN–GA3**.

The computed relative energies (ΔE), Gibbs free energies in vacuum under standard conditions ($\Delta G°$) as well as in aqueous solution ($\Delta G°_{aq}$) are compiled in Table 1. The data reveal that the thermal and entropy contributions to the absolute energies cause some changes in the relative energy values, but they do not change the order of relative stabilities. In contrast, the effect of aqueous media (estimated by the polarizable continuum model) results in dramatic changes in the relative stabilities. The polar medium seems to favour the CH_2OH orientation changed from ^4O towards ^5O (**GN–GA1** vs **GN–GA2)**, while in the β-(1→3) type the free character of the acetylamino group jointly with the turnover of the GN ring (**GA–GN5** vs **GA–GN1**) is preferred. The obtained preference of the **GA–GN5** structure in aqueous solution is in agreement with previous NMR studies on the salt in aqueous solution reporting an average (over the conformational equilibrium in the solution) $^1H\cdots{}^3H$ interglycosidic distance of 2.57 ± 0.08 Å.[11,41] Our computed value for **GA–GN5** is 2.28 Å.

3.2. Acids

Investigation of the acid forms of the disaccharides provides information on the effect of protonation in this type of compounds. The most stable acid conformers are shown in Figure 3 together with the characteristic hydrogen bonding interactions.

Similar to our observations on the anions, the acids do not show a distinguished preference of β-(1→4) or β-(1→3) linking either. The absolute energies of the two forms **GN–GAH** and **GAH–GN** are very close and the ordering is influenced by thermal, entropy and solvent effects. Among all the acidic forms the most stable structure is **GAH–GN1** in terms of potential and Gibbs free energies while **GN–GAH7** in terms of solvated Gibbs free energy.

From the **GN–GAH** species, eight conformers and from the **GAH–GN** species, six conformers fell in the Gibbs free energy window of 20 kJ/mol (Table 2). The individual conformers within the two types differ by weak interactions evolved by altered orientations of the CH_2OH, OCH_3, carboxyl and/or the acetylamino groups

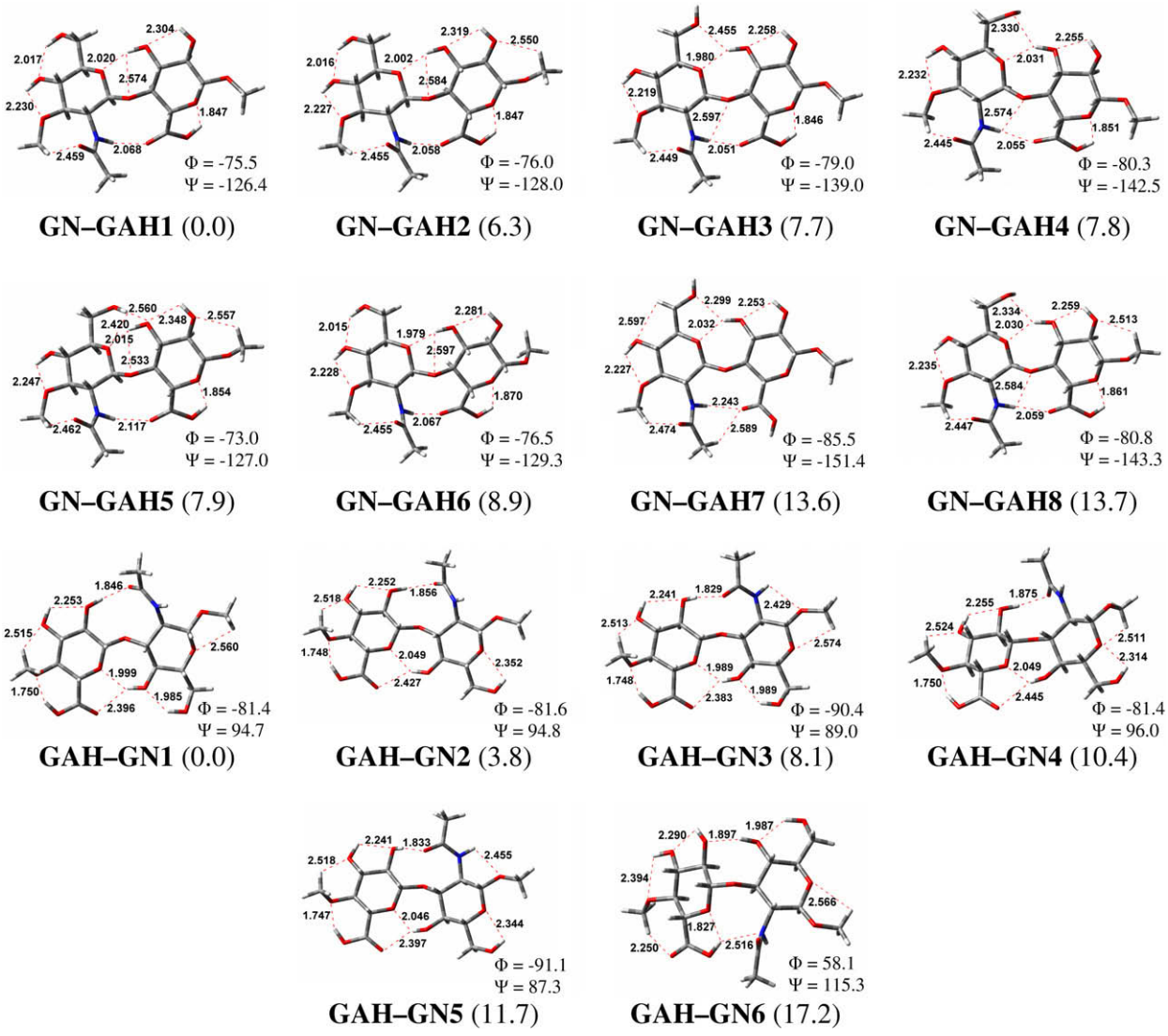

Figure 3. The most stable acid **GN–GAH** and **GAH–GN** disaccharides. The computed relative Gibbs free energies in vacuum (kJ/mol) are given in parentheses. The hydrogen bond distances are given in Å. The torsionals are defined as follows: $\Phi = {}^{7a}O–{}^{1a}C–{}^{8}O–{}^{3b}C$ and $\Psi = {}^{1a}C–{}^{8}O–{}^{3b}C–{}^{4b}C$ (for 1→3-linked disaccharides); $\Phi = {}^{7b}O–{}^{1b}C–{}^{8}O–{}^{4a}C$ and $\Psi = {}^{1b}C–{}^{8}O–{}^{4a}C–{}^{5a}C$ (for 1→4-linked disaccharides). For numbering of atoms see Figure 1.

Table 2
Computed relative energies (ΔE), Gibbs free energies in vacuum under standard conditions (ΔG^{o}) as well as in aqueous solution (ΔG°_{aq}) of the most stable anionic **GN–GAH** and **GAH–GN** disaccharides given in kJ/mol

Name	ΔE	ΔG°	ΔG°_{aq}
GN–GAH1	0.0	0.0	12.0
GN–GAH2	5.6	6.3	19.9
GN–GAH3	9.4	7.7	9.8
GN–GAH4	7.1	7.8	8.4
GN–GAH5	6.0	7.9	20.5
GN–GAH6	4.6	8.9	22.4
GN–GAH7	16.5	13.6	0.0
GN–GAH8	12.2	13.7	15.7
GAH–GN1	0.0	0.0	1.7
GAH–GN2	6.6	3.8	0.0
GAH–GN3	3.9	8.1	21.7
GAH–GN4	11.7	10.4	4.2
GAH–GN5	10.7	11.7	19.7
GAH–GN6	23.9	17.2	13.3

(see Fig .3). Note that the structures of lowest-energy acid disaccharides are very similar to those of the lowest-energy anions (cf. Figs. 2 and 3).

Experimental structural data for the neutral acid form of hyaluronan have been reported by Almond et al.[23] on the basis of solution NMR studies. The computed values for the β-(1→4) linkage of the most stable conformers in Figure 3 are in very good agreement with the experimental values (the deviations are within 10°), while the agreement for the β-(1→3) linkage is somewhat worse: the Φ and Ψ torsionals differ by 10° and 35°, respectively.[23] This means that the solvent effects do not change considerably the most stable relative orientations of the **GN** and **GAH** pyranose rings found for the isolated disaccharide structures by our computations.

Compared to the anions, the repertoire of hydrogen bonding in the acids is increased by the appearance of the carboxylic OH hydrogen. The diminished anionic character of the carboxyl group weakens its proton acceptor character, while the acidic carboxyl OH group is a strong proton donor. In most depicted conformers, this carboxylic OH group forms the shortest hydrogen bonds with lengths between 1.75 and 1.87 Å.

Beyond the bridging glycosidic oxygen, the **GN** and **GAH** moieties are connected by two-to-four hydrogen bonds from which the C=O···^{2}OH interactions in the **GAH–GN** structures are the strongest (1.83–1.88 Å). We can observe among these intermoiety interactions both bifurcated hydrogen bonds and weaker CH···O interactions. The structure of **GAH–GN6** differs from the other **GAH–GN** structures by its **GN** ring turned over with respect to the **GA** moiety. The role of steric and other minor interactions is shown by the somewhat higher energy of **GAH–GN5** with respect to **GAH–GN2**. The two structures differ by an ∼90° rotation of the acetylamino group resulting in slightly shorter hydrogen bonds in **GAH–GN5**. This stronger hydrogen bonding, however, seems to be overcompensated by the sum of other weak interactions favouring **GAH–GN2**.

The computed energy data of the **GN–GAH** and **GAH–GN** disaccharides are compiled in Table 2. Similarly to the experience on the anionic disaccharides shown above, there are some minor changes in the stability order between the potential and Gibbs free energies. Again, the strongly polar aqueous media result in considerable changes in the relative stabilities. We want to emphasize here the dramatic stabilization of **GN–GAH7** in aqueous solution, which is the result of the completely free COOH group in this structure (the only one within the 20 kJ/mol window presented in Figure 2). At the same time, the **GN–GAH1** and **GN–GAH2** conformers (most stable in the gaseous phase) are considerably destabilized in solution.

3.3. Sodium salts

Hyaluronan exerts its biological functions in the human body mainly in the form of sodium salt, hence we paid particular attention to this form in our comparative study. Our modelling, however, had the limitation of treating the Na^{+} cation within the isolated disaccharide moiety, whereas its arrangement in real systems is somewhat different. In the solid phase, Na^{+} ions bridge neighbouring hyaluronan chains, while in aqueous solution it is generally separately solvated by the solvent molecules. However, in the dynamic solvation process hyaluronan···Na^{+} adducts have also some relevance. The following computed results give valuable information on the bonding interactions (type and strength) of Na^{+} with hyaluronan.

The most stable salt conformers are depicted in Figure 4 together with the Na···O and intramolecular hydrogen bonding interactions. The energy data are compiled in Table 3. Compared to the anions and neutral disaccharides, there are less low-energy conformers among the sodium salts. Therefore, only three conformers fitted in the 20 kJ/mol ΔG^{o} window from each of the β-(1→4) and β-(1→3) type disaccharides. The global minimum on the potential energy surface of the sodium salt was **GN–GANa1** in terms of both ΔE and ΔG^{o}. Similarly to the anions and neutral acids discussed above the β-(1→3) type, **GANa–GN1**, is very close in energy (within 3 kJ/mol). Dramatic changes were introduced by the solvent, which stabilized considerably the **GANa–GN5** and **GN–GANa17** structures. From the two linking types **GN–GANa17** is lower in energy by 8.2 kJ/mol.

The main question regarding these structures is the position of the Na^{+} ion. As can be expected from the strongly charged character of the carboxylate group, it forms an ion pair with Na^{+}···O distances between 2.14 and 2.24 Å (cf. Fig. 4). These distances agree very well with the Na^{+}···O distance computed recently for isolated sodium acetate (2.207 Å).[52] In the investigated disaccharide structures, the Na^{+} ion is involved in secondary interactions with other close lying oxygens (either with OH oxygens or with the amide oxygen in **GANa–GN2**, **GN–GANa1** and **GN–GANa3**). As a consequence, Na^{+} is positioned asymmetrically near the carboxylate group, the most extreme case being **GANa–GN2** where it is connected only to one of the carboxylate oxygens. While these secondary interactions do not seem to affect the Na^{+}···carboxylate interaction considerably (vide supra the comparison with sodium acetate), they seem to be quite strong as indicated by the Na^{+}···O distances of 2.2–2.5 Å.

The Φ and Ψ torsionals of the most stable **GN–GANa1** and **GANa–GN1** structures are in good agreement (deviations of 10–30°) with the X-ray diffraction results on the sodium hyaluronate salts.[18,19] The agreement is particularly remarkable considering the somewhat different position of the Na^{+} ions in the crystal and computed structures (in the crystal the Na^{+} ions are positioned between hyaluronan chains, while in the computed structures they are localized around a single carboxylate group). This refers to the importance of the other (secondary) interactions regarding the relative arrangement of the **GN** and **GAH** pyranose rings. A similar situation was observed upon comparison with NMR data.[11]

Salt formation rearranges the hydrogen bonds in the vicinity of the carboxylate group, but it has no systematic effect on the other hydrogen bonds. Analyzing the structural and energetic information depicted in Figure 4, we can say that the relative stabilities of the various conformers have no direct dependence on the number and strength of the Na^{+} ion interactions. The entire hydrogen bonding network, steric and other weak interactions remain important factors for the relative stabilities. The differences in weak interactions upon rotation of the methoxy group in the **GA** moiety (CH···O hydrogen bond, dipole–dipole and steric effects)

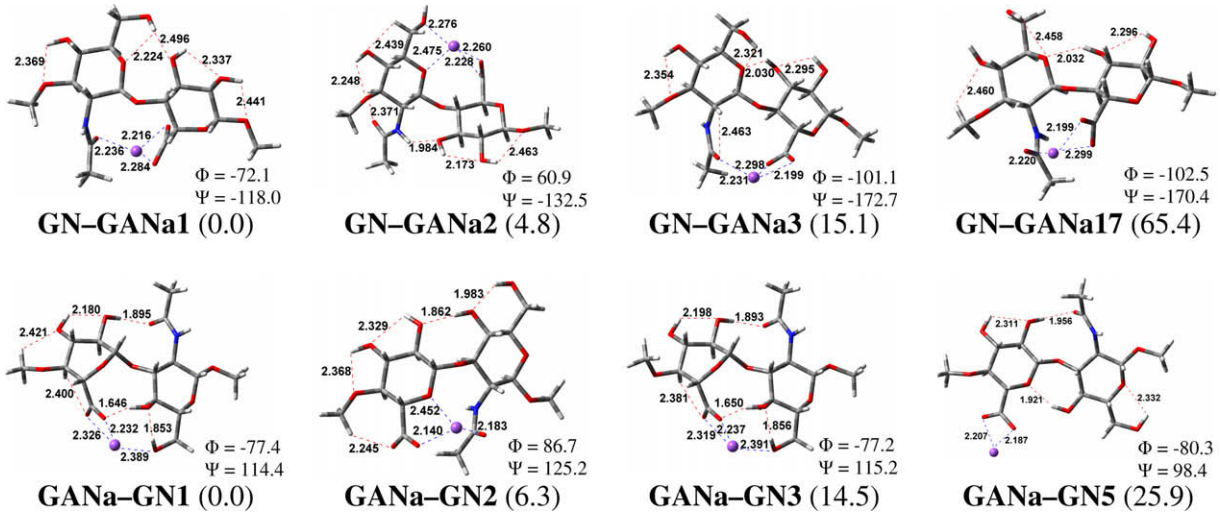

Figure 4. The most stable salt **GN–GANa** and **GANa–GN** disaccharides. The computed relative Gibbs free energies in vacuum (kJ/mol) are given in parentheses. The Na···O and hydrogen bond distances are given in Å. The torsionals are defined as follows: $\Phi = {}^{7a}O{-}{}^{1a}C{-}{}^{8}O{-}{}^{3b}C$ and $\Psi = {}^{1a}C{-}{}^{8}O{-}{}^{3b}C{-}{}^{4b}C$ (for 1→3-linked disaccharides); $\Phi = {}^{7b}O{-}{}^{1b}C{-}{}^{8}O{-}{}^{4a}C$ and $\Psi = {}^{1b}C{-}{}^{8}O{-}{}^{4a}C{-}{}^{5a}C$ (for 1→4-linked disaccharides). For numbering of atoms see Figure 1.

Table 3
Computed relative energies (ΔE), Gibbs free energies in vacuum under standard conditions (ΔG°) as well as in aqueous solution (ΔG°_{aq}) of the most stable **GN–GANa** and **GANa–GN** disaccharides given in kJ/mol

Name	ΔE	ΔG°	ΔG°_{aq}
GN–GANa1	0.0	0.0	4.5
GN–GANa2	5.7	4.8	12.8
GN–GANa3	16.1	15.1	6.3
GN–GANa17	68.4	65.4	0.0
GANa–GN1	0.0	0.0	34.4
GANa–GN2	10.9	6.3	24.4
GANa–GN3	13.0	14.5	43.8
GANa–GN5	40.9	25.9	0.0

add up to a destabilization by 14.5 kJ/mol observed between the **GANa–GN1** and **GANa–GN3** conformers.

Another noteworthy observation is that the pyranose ring of the **GA** moiety of **GANa–GN1** and **GANa–GN3** turned into the twist form during our geometry optimization to avoid the steric repulsion between the bridging glycosidic oxygen and the ring oxygen of **GA** (Due to this steric repulsion the $^4C_1$ chair is not a stationary point on the potential energy surface in these cases.) The turnover facilitated the approach of the two rings required for the optimal interactions of the Na^+ ion. As stated in the introduction, our study is focussed on the $^4C_1$ chair pyranose rings present in hyaluronan; therefore, we omitted a detailed investigation of the other ring conformers. We performed only a few test calculations and found, when both the $^4C_1$ and twist ring conformers are minima, they are generally close (2–5 kJ/mol) in energy.

The effect of aqueous solvent among all our investigated compounds is most pronounced for the salts. It destabilizes particularly the most stable isolated **GANa–GN** structures (Table 3).

3.4. Effect of protonation and salt formation on the structural properties

The model structures of the following discussion have been obtained by subsequent geometry optimizations starting from the most stable anions **GN–GA1** and **GA–GN1**, protonating their COO groups and afterwards replacing the COOH hydrogen with Na in the optimized acid structures. It should be noted that in some cases the obtained structures are quite high in energy and these were not included in the previous discussions of the most stable conformers. On the other hand, they reflect the independent effects of protonation and salt formation, being the subject of this section.

Comparing the protonated forms of the hyaluronan disaccharides with the anions we can see differences mainly in the vicinity of the carboxylate group. We discuss in detail first the **GN–GA1**/**GN–GAH1** pair, both being the global minima on the Gibbs free energy surface in vacuum (the other acid–anion pairs show similar features). The main difference in the two structures is the rotation of the COO group by 75° (see Fig. 5). The strong COO···HN hydrogen bond (1.774 Å) and weak COO···H_3C interaction (2.335 Å) in **GN–GA1** are replaced by the somewhat weaker COOH···^{5}O (1.847 Å) and COO···HN (2.068 Å) hydrogen bonds in **GN–GAH1** (Figs. 2 and 3). Replacement of the COOH hydrogen by sodium results in a single considerable change in the geometry: it is the rotation of the OCH_3 group driven by the formed attractive electrostatic interaction between its oxygen and Na^+ (see Fig. 5). In this structure, the Na^+ ion is connected to the **GA** moiety by the ionic bond with the carboxylate and two weaker electrostatic interactions with the ring and OCH_3 oxygens. Note that this structure is in the fourth place in the energy order of the salts, being higher by 27.7 kJ/mol than the most stable **GN–GANa1** structure.

Regarding the electron density distribution, noticeable changes happen only in the vicinity of the COO group upon the protonation. The formation of the COOH group changes considerably the charge of the non-protonated COO oxygen (from −0.80 to −0.62 e), while the negative charge of the protonated COO oxygen decreases by 0.03 e only (Fig. 5). An increase in a similar magnitude (0.04 e) appears at the ring oxygen, which is involved in a weak hydrogen bonding interaction with the COOH hydrogen in **GN–GAH1**. Larger changes in this part of the molecule can be observed in the sodium salt. The natural charge of Na is around +0.9 in these compounds, hence its interaction with the near-lying oxygens is strongly ionic. These stronger electrostatic interactions of Na^+ result in considerable increase of negative charges on the connecting carboxyl, ring and OCH_3 oxygens. Another noteworthy effect is the inverse electron density distribution within the COO group going from **GN–GA1** to **GN–GANa4**, which weakens also the CO···HN hydrogen bond with respect to that in the anion (1.889 vs 1.774 Å).

In the case of the **GA–GN**, **GAH–GN** and **GANa–GN** structures, the protonation results in much larger changes of the stability order than observed in the case of the **GN–GA** models (vide supra).

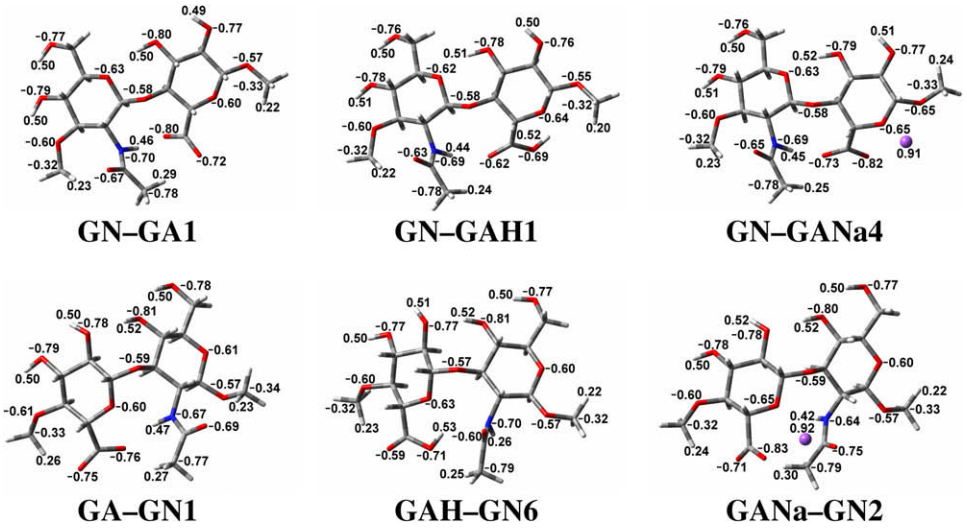

Figure 5. Comparison of the natural atomic charges in selected structures.

We compare here the lowest-energy **GA–GN1** conformer with its acid pair **GAH–GN6**, which is higher in energy by 17.2 kJ/mol than the global minimum **GAH–GN1**. The most drastic structural change between **GA–GN1** and **GAH–GN6** is the break of the strong CO···HN hydrogen bond, as the respective COO oxygen gets protonated. To avoid the steric repulsion of the NH and COOH groups, the acetylamino group rotated by ca. 90° and is not involved in any intramolecular hydrogen bond in the **GAH–GN6** local minimum structure. The rest of the molecule does not show any considerable structural change. The other hydrogen bonding interactions remain intact, and the only new hydrogen bond is that formed between the COOH hydrogen and the ring O of the **GAH** moiety. Replacement of the COOH hydrogen with Na^+ in **GANa–GN2** keeps the acetylamino group in the rotated position present also in **GAH–GN6**. In **GANa–GN2** the Na^+ ion forms a bifurcated ionic interaction with the COO group on one side and CO of the acetylamino group on the other side. Both acceptor groups are rotated into an appropriate position for this interaction, being the only major changes in the structure.

The natural charges show the same characteristics discussed above for the **GN–GA** models. Considerable changes appear only in the vicinity of the breaking and forming interactions, in a similar magnitude like that in the **GN–GA** models (vide supra).

4. Conclusion

In the present paper we reported our results on the conformational properties of β-(1→4) and β-(1→3)-linked disaccharides of hyaluronan. The study was restricted to the $^4C_1$ chair forms of the monosaccharide skeletons, found in crystal structure studies. We studied the isolated anions, neutral acids and sodium salts, and their comparative analysis provided information on the structural effect of protonation and salt formation.

We found that the most stable conformers of the isolated anion and acid are those possessing the largest number of strong hydrogen bonds. Hence, the intramolecular hydrogen bonding interactions represent the main stabilizing forces for the conformers. The exact stability order, however, is also influenced by additional weak interactions (dipole–dipole, charge transfer, steric) that can even fortuitously add up to overcompensate the effect of a hydrogen bond. We showed representative examples for this phenomenon.

The protonation and salt formation change the hydrogen bonding in the vicinity of the carboxyl group, resulting in most cases in a considerable alteration of the conformational preferences. The Na^+ ion is connected primarily to the carboxylate group, but in addition it forms slightly weaker interactions with neighbouring oxygens. Analysis of the natural charges indicated that the main effect of protonation and salt formation on the electron density distribution is restricted on the surroundings of the broken/formed interactions near the carboxylate group.

The effect of water solvent was assessed using the PCM-polarized continuum model. Although this model neglects the important explicit interaction with the solvent water molecules, our results could indicate the trends of changing conformational preferences in the solution. Those structures get considerably stabilized by the solvent, of which highly polar groups (CH_2OH, COO, NHCO) get partly or completely released from the intramolecular hydrogen bonding network.

Acknowledgements

This research was initiated by Professor István Hargittai and we thank him for his advice and discussion. We gratefully acknowledge the financial support from the Hungarian Scientific Research Foundation (OTKA No. T046183) and computational time from the National Information Infrastructure Development Program of Hungary.

Supplementary data

Supplementary data associated with this article can be found, in the online version, at doi:10.1016/j.carres.2009.05.030.

References

1. The Biology of Hyaluronan, Ciba Foundation Symposium 143, 1989.
2. Stern, R.; Asari, A. A.; Sugahara, K. N. *Eur. J. Cell Biol.* **2006**, *85*, 699–715.
3. Scott, J. E. *Biorheology* **2008**, *45*, 209–217.
4. Balazs, E. A. *Curr. Pharm. Biotechnol.* **2008**, *9*, 236–238.
5. Hargittai, I.; Hargittai, M. *Struct. Chem.* **2008**, *19*, 697–717.
6. Almond, A. *Cell. Mol. Life Sci.* **2007**, *64*, 1591–1596.
7. Cowman, M. K.; Matsuoka, S. *Carbohydr. Res.* **2005**, *340*, 791–809.
8. Lapcik, L., Jr.; Lapcik, L.; De Smedt, S.; Demeester, J.; Chabrecek, P. *Chem. Rev.* **1998**, *98*, 2663–2684.
9. Laurent, T. C.; Laurent, U. B. G.; Fraser, J. R. E. *Immunol. Cell. Biol.* **1996**, *74*, A1–A7.
10. Atkins, E. D. T.; Meader, D.; Scott, J. E. *J. Biol. Macromol.* **1980**, *2*, 318–319.
11. Holmbeck, S. M. A.; Petillo, P. A.; Lerner, L. E. *Biochemistry* **1994**, *33*, 14246–14255.
12. Scott, J. E. *FASEB J.* **1992**, *6*, 2639–2645.

13. Mitra, A. K.; Arnott, S.; Sheehan, J. K. *J. Mol. Biol.* **1983**, *169*, 813–827.
14. Mitra, A. K.; Raghunathan, S.; Sheehan, J. K.; Arnott, S. *J. Mol. Biol.* **1983**, *169*, 829–859.
15. Arnott, S.; Mitra, A. K.; Raghunathan, S. *J. Mol. Biol.* **1983**, *169*, 861–872.
16. Sheeehan, J. K.; Gardner, K. H.; Atkins, E. D. T. *J. Mol. Biol.* **1977**, *117*, 113–135.
17. Winter, W. T.; Arnott, S. *J. Mol. Biol.* **1977**, *117*, 761–784.
18. Winter, W. T.; Smith, P. J. C.; Arnott, S. *J. Mol. Biol.* **1975**, *99*, 219–235.
19. Guss, J. M.; Hukins, D. W. L.; Smith, P. J. C.; Winter, W. T.; Arnott, S. *J. Mol. Biol.* **1975**, *95*, 359–384.
20. Dea, I. C. M.; Moorhouse, R.; Rees, D. A.; Arnott, S.; Guss, J. M.; Balazs, E. A. *Science* **1973**, *179*, 560–562.
21. Atkins, E. D. T.; Sheehan, J. K. *Science* **1973**, *179*, 562–564.
22. Atkins, E. D. T.; Sheehan, J. K. *Nat. New Biol.* **1972**, *235*, 253–254.
23. Almond, A.; DeAngelis, P. L.; Blundell, C. D. *J. Mol. Biol.* **2006**, *358*, 1256–1269.
24. Blundell, C. D.; Reed, M. A. C.; Almond, A. *Carbohydr. Res.* **2006**, *341*, 2803–2815.
25. Almond, A.; Colebrooke, S. A.; DeAngelis, P. L.; Mahoney, D. J.; Day, A. J.; Blundell, C. D. Dynamic Conformational Predictions for Hyaluronan: Using NMR to Confirm Aqueous Simulations. In *Hyaluronan: Structure, Metabolism, Biological Activities, Therapeutic Applications*; Balazs, E. A., Hascall, V. C., Eds.; Matrix Biology Institute: Edgewater, NJ, 2005; pp 3–6.
26. Donati, A.; Magnani, A.; Bonechi, C.; Barbucci, R.; Rossi, C. *Biopolymers* **2001**, *59*, 434V445.
27. Cavalieri, F.; Chiessi, E.; Paci, M.; Paradossi, G.; Flaibani, A.; Cesaro, A. *Macromolecules* **2001**, *34*, 99V109.
28. Cowman, M. K.; Feder-Davis, J.; Hittner, D. M. *Macromolecules* **2001**, *34*, 110V115.
29. Cowman, M. K.; Hittner, D. M.; Feder-Davis, J. *Macromolecules* **1996**, *29*, 2894–2902.
30. Bayraktar, H.; Akal, E.; Sarper, O.; Varnali, T. *J. Mol. Struct. (Theochem)* **2004**, *683*, 121–132.
31. Tafi, A.; Manetti, F.; Corelli, F.; Alcaro, S.; Botta, M. *Pure Appl. Chem.* **2003**, *75*, 359–366.
32. Almond, A.; Sheehan, J. K. *Glycobiology* **2003**, *13*, 255–264.
33. Sheehan, J.; Almond, A. Hyaluronan: Static, Hydrodynamic and Molecular Dynamic Views. In *Glyocoforum:Hyaluronan Today*; Hascall, V. C., Yanagishita, M., Eds.; Seikagaku Corporation Gycoforum, 2001.
34. Haxaire, K.; Braccini, I.; Milas, M.; Rinuado, M.; Pérez, S. *Glycobiology* **2000**, *10*, 587–594.
35. Kaufmann, J.; Möhle, K.; Hofmann, H. J.; Arnold, K. *J. Mol. Struct. (Theochem)* **1998**, *422*, 109–121.
36. Almond, A.; Brass, A.; Sheehan, J. K. *Glycobiology* **1998**, *8*, 973–980.
37. Almond, A.; Brass, A.; Sheehan, J. K. *J. Mol. Biol.* **1998**, *284*, 1425–1437.
38. Almond, A.; Sheehan, J. K.; Brass, A. *Glycobiology* **1997**, *7*, 597–604.
39. Mo, F.; Jensen, L. H. *Acta Crystallogr., Sect. B* **1975**, *31*, 2867–2873.
40. Moulabbi, M.; Broch, H.; Robert, L.; Vasilescu, D. *J. Mol. Struct. (Theochem)* **1997**, *395*, 477–508.
41. Miertus, S.; Bella, J.; Toffanin, R.; Matulova, M.; Paoletti, S. *J. Mol. Struct. Theochem.* **1997**, *395*, 437–449.
42. Nyerges, B.; Kovács, A. *J. Phys. Chem. A* **2005**, *109*, 892–897.
43. Frisch, M. J.; Trucks, G. W.; Schlegel, H. B.; Scuseria, G. E.; Robb, M. A.; Cheeseman, J. R.; Montgomery Jr., J. A.; Vreven, T.; Kudin, K. N.; Burant, J. C.; Millam, J. M.; Iyengar, S. S.; Tomasi, J.; Barone, V.; Mennucci, B.; Cossi, M.; Scalmani, G.; Rega, N.; Petersson, G. A.; Nakatsuji, H.; Hada, M.; Ehara, M.; Toyota, K.; Fukuda, R.; Hasegawa, J.; Ishida, M.; Nakajima, T.; Honda, Y.; Kitao, O.; Nakai, H.; Klene, M.; Li, X.; Knox, J. E.; Hratchian, H. P.; Cross, J. B.; Bakken, V.; Adamo, C.; Jaramillo, J.; Gomperts, R.; Stratmann, R. E.; Yazyev, O.; Austin, A. J.; Cammi, R.; Pomelli, C.; Ochterski, J. W.; Ayala, P. Y.; Morokuma, K.; Voth, G. A.; Salvador, P.; Dannenberg, J. J.; Zakrzewski, V. G.; Dapprich, S.; Daniels, A. D.; Strain, M. C.; Farkas, O.; Malick, D. K.; Rabuck, A. D.; Raghavachari, K.; Foresman, J. B.; Ortiz, J. V.; Cui, Q.; Baboul, A. G.; Clifford, S.; Cioslowski, J.; Stefanov, B. B.; Liu, G.; Liashenko, A.; Piskorz, P.; Komaromi, I.; Martin, R. L.; Fox, D. J.; Keith, T.; Al-Laham, M. A.; Peng, C. Y.; Nanayakkara, A.; Challacombe, M.; Gill, P. M. W.; Johnson, B.; Chen, W.; Wong, M. W.; Gonzalez, C.; Pople, J. A. GAUSSIAN *03, Revision D.01*, Gaussian: Wallingford, CT, 2004.
44. Becke, A. D. *J. Chem. Phys.* **1993**, *98*, 5648–5652.
45. Lee, C.; Yang, W.; Parr, R. G. *Phys. Rev. B* **1988**, *37*, 785–789.
46. Cossi, M.; Barone, V.; Cammi, R.; Tomasi, J. *Chem. Phys. Lett.* **1996**, *255*, 327–335.
47. Cammi, R.; Mennucci, B.; Tomasi, J. *J. Phys. Chem. A* **2000**, *104*, 5631–5637.
48. Cossi, M.; Scalmani, G.; Rega, N.; Barone, V. *J. Chem. Phys.* **2002**, *117*, 43–54.
49. Glendening, E. D.; Badenhoop, J. K.; Reed, A. E.; Carpenter, J. E.; Bohmann, J. A.; Morales, C. M.; Weinhold, F. *NBO 5.0*; Theoretical Chemistry Institute, University of Wisconsin: Madison, 2001.
50. Furlan, S.; La Penna, G.; Perico, A.; Cesàro, A. *Carbohydr. Res.* **2005**, *340*, 959–970.
51. Almond, A.; Brass, A.; Sheehan, J. K. *J. Phys. Chem. B* **2000**, *104*, 5634–5640.
52. Remko, M.; Hricovíni, M. *Struct. Chem.* **2007**, *18*, 537–547.